The Astrophysical Journal, 673: L95–L98, 2008 January 20

ACCELERATION IN FAST HALO CMEs AND SYNCHRONIZED FLARE HXR BURSTS

M. Temmer
Hvar Observatory, Faculty of Geodesy, University of Zagreb, Kačićeva 26, HR-10000 Zagreb, Croatia; mat@igam.uni-graz.at
A. M. Veronig
IGAM/Kanzelhöhe Observatory, Institute of Physics, Universität Graz, Universitätsplatz 5, A-8010 Graz, Austria
B. Vršnak
Hvar Observatory, Faculty of Geodesy, University of Zagreb, Kačićeva 26, HR-10000 Zagreb, Croatia
J. Rybák and P. Gömöry
Astronomical Institute/SAS, SK-05960 Tatranská Lomnica, Slovakia
S. Stoiser
IGAM/Kanzelhöhe Observatory, Institute of Physics, Universität Graz, Universitätsplatz 5, A-8010 Graz, Austria
and
D. Maričić
Hvar Observatory, Faculty of Geodesy, University of Zagreb, Kačićeva 26, HR-10000 Zagreb, Croatia
Received 2007 September 25; accepted 2007 December 3; published 2008 January 8

ABSTRACT

We study two well-observed, fast halo CMEs, covering the full CME kinematics including the initiation and impulsive acceleration phase, and their associated flares. We find a close synchronization between the CME acceleration profile and the flare energy release as indicated by the *RHESSI* hard X-ray flux onsets, as well as peaks occur simultaneously within 5 minutes. These findings indicate a close physical connection between both phenomena and are interpreted in terms of a feedback relationship between the CME dynamics and the reconnection process in the current sheet beneath the CME.

Subject headings: Sun: coronal mass ejections (CMEs) — Sun: flares — Sun: X-rays, gamma rays

Online material: color figures

1. INTRODUCTION

Coronal mass ejections (CMEs) are closely related to solar flares as well as filament eruptions. In the "standard" model, the erupting filament or CME stretches the coronal magnetic field lines to build up a vertical current sheet where magnetic reconnection sets in and releases vast amounts of energy (e.g., Forbes 2000). A few observational studies compare the full CME kinematics and the energy release in the associated flare, using the *GOES* soft X-ray flux derivative as a flare indicator, and LASCO C1 or Mauna Loa MK4 coronagraphs for observing the CME evolution in the low corona down to $\sim$1.1 $R_\odot$ (Zhang et al. 2001, 2004; Vršnak et al. 2004; Maričić et al. 2007). For a substantial fraction of the studied events, a close relationship between both phenomena was found. The main problem for conducting such studies is that the impulsive CME acceleration (main acceleration) takes place in the inner corona, $R \lesssim 3\ R_\odot$ (MacQueen & Fisher 1983; St. Cyr et al. 1999; Vršnak 2001), which is difficult to observe using coronagraphs. However, this phase is the most interesting one for the CME dynamics, since in the outer corona the CMEs might be already adjusted to the solar wind speed or show just some "residual acceleration" (Chen & Krall 2003; Zhang & Dere 2006). Only a few studies compared directly the kinematics of prominence/filament eruptions and associated HXR bursts (Kahler et al. 1988; Sterling & Moore 2004, 2005). However, prominences/filaments do not represent the leading edge of CMEs, and their dynamical evolution might be different. Only in one event (Sterling & Moore 2004) were the height-time measurements from the filament's overlying loops measured and compared to the flare HXRs; however, the sampling during the main acceleration phase was not sufficient to derive a reliable acceleration profile.

In this respect it should be noted that also the kinematics of X-ray plasmoids was compared to HXR bursts, and in some cases a temporal correlation was found (e.g., Ohyama & Shibata 1997, 1998). However, X-ray plasmoids generally do not represent the early signature of a CME's leading edge but sometimes just form by tearing of the current sheet in the course of the flaring process beneath the CME (Shibata & Tanuma 2001), so various types of relations were observed (for details see Kim et al. 2005).

Front-sided, fast halo CMEs are the most geo-effective CMEs (e.g., Zhang et al. 2003) and are thus vitally important to study. However, they are most difficult to measure: "Fast" implies that a good imaging cadence is needed to properly characterize their dynamical evolution. "Halo" implies that the CME source region is located centrally on the solar disk. This means that a considerable part of the early CME evolution appears against the solar disk; i.e., it cannot be observed by coronagraphs. Therefore, it is important to identify CME structures in on-disk coronal images (see studies by Hudson et al. 1996; Dere et al. 1997; Alexander et al. 2002; Gallagher et al. 2003; Uralov et al. 2005; Vršnak et al. 2006; Dauphin et al. 2006).

Here we present a detailed study of the full kinematics of two well-observed, fast halo CMEs and their associated flares. On-disk CME signatures are identified and measured in SXI, *TRACE*, and EIT images with high time cadence, which enables us to study the CME initiation and acceleration. The impulsive phase of the associated flares is fully covered by *RHESSI* hard X-ray observations. Flare hard X-rays are due to fast electrons and provide the most direct indicator of the evolution of the energy release in the flare. This is the first time that the full kinematics of fast halo CMEs is compared with the flare hard X-ray bursts.

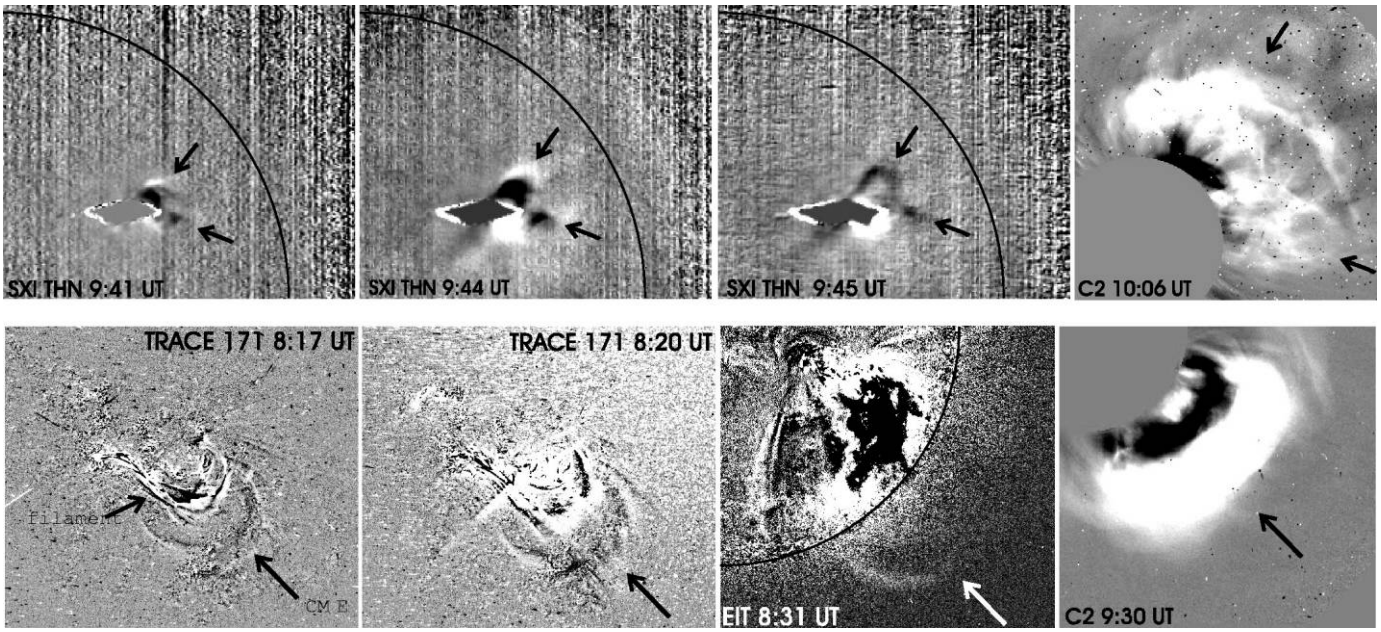

FIG. 1.—*Top*: 2005 January 17 CME. Sequence of three SXI running ratio images and one LASCO C2 running difference image. *Bottom*: 2006 July 6 CME. Sequence of two *TRACE* 171 Å, one EIT 195 Å, and one LASCO C2 running difference images.

2. OBSERVATIONS

2.1. *2005 January 17: X3.8 Flare/CME Event*

The fast CME of 2005 January 17 was associated with an X3.8/3B flare at heliographic position N15°, W25°. *RHESSI* (Lin et al. 2002) covered the full impulsive phase of the event, with several strong HXR bursts over a period of ~30 minutes. Details on the flare aspect can be found in Veronig et al. (2006) and Temmer et al. (2007).

The associated CME was observed with the Large Angle and Spectrometric Coronagraph (LASCO; Brueckner et al. 1995) instruments C2 and C3 on the *Solar and Heliospheric Observatory* (*SOHO*), which have a field of view (FOV) of 2–6 and 6–30 $R_\odot$, respectively. It appeared as a fast halo CME (360° angular width, but most pronounced in the northwest quadrant) with a linear plane-of-sky speed of ~2000 km s^{-1} in the LASCO FOV. The early, on-disk evolution of the CME could be observed with the *GOES 12* Solar X-Ray Imager (SXI; Hill et al. 2005). Rising looplike structures could be identified in nine SXI frames with a time cadence of ~2–4 minutes and a spatial resolution of 5″ pixel^{-1} (cf. top row of Fig. 1).

Although it is not apriori clear how the hot, X-ray–emitting plasma observed with SXI relates to the CME plasma observed in scattered white light with LASCO, there is indication that the rising SXI loops are part of the CME: The eruption observed in SXI against the solar disk consists of two evolving elements that propagate toward the northwest and west, respectively. The same two-part morphology and propagation directions are observed in LASCO C2 images (see Fig. 1, *top row*). In addition, since no filament was observed in Hα prior and/or erupting during the flare, it is unlikely that the rising SXI features show an erupting filament.

2.2. *2006 July 6: M2.5 Flare/CME Event*

The CME of 2006 July 6 was associated with an M2.5/2N flare at heliographic position S9°, W34°. The *RHESSI* light curve of the associated flare shows several HXR bursts above 30 keV. The CME was observed in LASCO C2 and C3 as a halo CME (most prominent in the southwest quadrant) with a linear plane-of-sky velocity of ~900 km s^{-1}. On-disk CME signatures were observed in seven frames of the 171 Å EUV channel ($T \sim 1$ MK) of the *Transition Region and Coronal Explorer* (*TRACE*; Handy et al. 1999) with a time cadence of ~1.5–3 minutes and 0.5″ pixel^{-1} resolution during JOP176. In one frame, the CME signature was observed over the limb by the 195 Å filter ($T \sim 1.5$ MK) of the Extreme-ultraviolet Imaging Telescope (EIT; Delaboudinière et al. 1995) on board *SOHO*. The EIT images have a resolution of 2.6″ pixel^{-1} and a FOV extending to 1.4 $R_\odot$.

The bottom row of Figure 1 shows two *TRACE* images of the rising CME loops against the solar disk, one EIT image where the loops already extend over the solar limb, and a LASCO/C2 image of the CME. The direction as well as the morphology of the *TRACE* and EIT loops are in good consistency with the CME observed in white light by C2, which we take as evidence that *TRACE* and EIT indeed observe part of the CME structure. The *TRACE* images show embedded within the rising loops an erupting filament. The position of the erupting filament is clearly separated (~70″) from the overlying rising loops and is part of the CME later observed by LASCO.

3. METHODS

In order to determine the distance-time profiles for the CMEs under study, we derived for each observational data set running difference (in case of SXI also running ratio) images between subsequent frames and measured at each instant the leading edge (LE) positions of the "white" evolving features, i.e., the outermost front of the observed CME structure. For the SXI data set (2005 January 17 event), we also measured the outer edge of the "black" feature (cf. Fig. 1), which roughly corresponds to the white feature in the previous difference image, and used the time tag of the subtracted image. With this method, we could follow the early CME evolution in nine SXI images, whereas the white feature was observed in only eight frames, and we could also cross-check the uncertainties of our measurements.

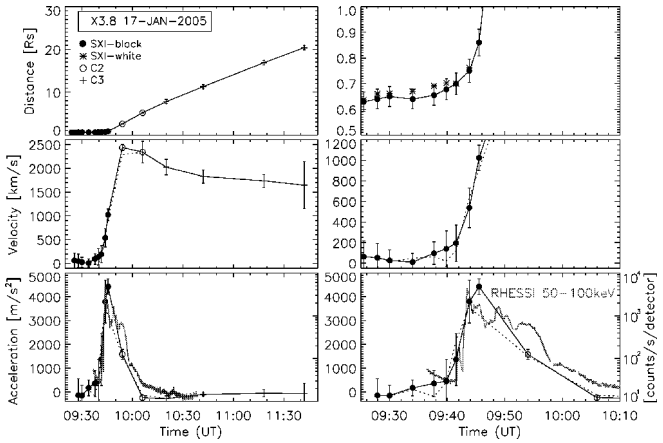

FIG. 2.—Event of 2005 January 17. From top to bottom, distance-time profile $d(t)$, velocity $v(t)$, and acceleration $a(t)$ of the CME as observed by different instruments (different plot symbols specified in the legend). In the bottom panel, we plot also the *RHESSI* 50–100 keV HXR flux of the associated flare. The left panels show the full CME height range covered by the LASCO FOV, i.e., up to 30 $R_\odot$. The right panels zoom into the early acceleration phase of the CME as observed against the solar disk in SXI. The solid curves connects the black features measured in the SXI running ratio images and subsequent LASCO measurements, the dashed curves refer to the white features. [*See the electronic edition of the Journal for a color version of this figure.*]

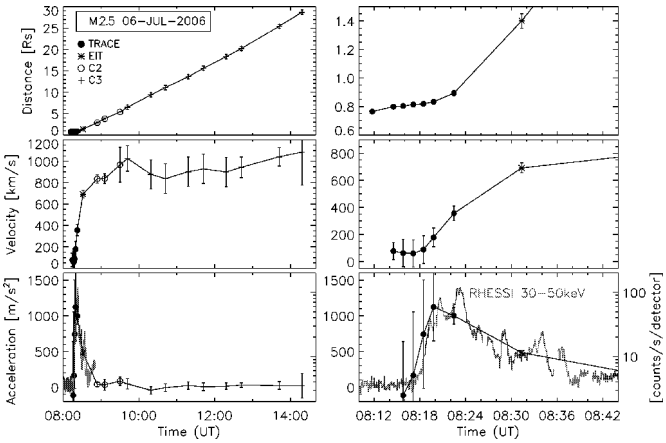

FIG. 3.—Same as Fig. 2, but for the 2006 July 6 event. In the bottom panel, we plot also the *RHESSI* 30–50 keV HXR flux of the associated flare. The left panels show the full CME height range covered by the LASCO FOV. The right panels zoom into the early acceleration phase of the CME as observed by *TRACE* and EIT. [*See the electronic edition of the Journal for a color version of this figure.*]

From this raw distance-time measurements, $d(t)$, we derived the CME plane-of-sky[1] velocity $v(t)$ and acceleration $a(t)$ profiles by numerical derivative methods (analogous to the procedure used in Zhang et al. 2004). We used a Lagrangian interpolation over three neighboring points before calculating the first and second derivative at any given $d(t)$ data point. To estimate the LE measurement uncertainties in the different data sets, we applied several independent measurements, and obtained typical uncertainties of ± 0.015, ± 0.04, ± 0.05, ± 0.1, and ± 0.5 $R_\odot$ for *TRACE*, SXI, EIT, C2, and C3 images, respectively.

4. RESULTS

Figure 2 shows the derived kinematics for the event of 2005 January 17. We show (*from top to bottom*) the time-distance measurements $d(t)$ of the CME LE as observed in SXI and LASCO C2 and C3 images, the velocity $v(t)$, and the acceleration $a(t)$ together with the *RHESSI* HXR flux. In our measurements, we followed the main CME element that propagated into the northwest direction (cf. Fig. 1, *top row*). The left panels show the whole CME evolution, i.e., from its early phase as observed on-disk in SXI images up to the full LASCO FOV of 30 $R_\odot$. The right panels show the same curves but focus on the early CME evolution in the inner corona, where the main acceleration takes place. The main acceleration starts around 09:40–09:42 UT, has a peak of 4.4 ± 0.3 km s^{-2} at 09:46 UT, and ends at ~10:06 UT. If we follow the white features in the SXI running difference images, then the acceleration peak occurs about 2 minutes earlier with a peak value of 3.5 ± 0.3 km s^{-2}.

It is worth noting that the kinematical curves derived from the white and black features in the SXI running ratio images are consistent with each other within the given limitations of the measurements. We also note that, although we have an exceptionally good coverage of the acceleration phase of this extremely fast CME in nine SXI frames, it is still not ideally covered. There is a gap of ~8 minutes between the last SXI data point and the first LASCO C2 data point. Therefore, we have to consider that the CME acceleration peak could happen a few minutes later than we derived.

The *RHESSI* 50–100 keV HXR flux of the associated X3.8 flare shows an impulsive increase at 09:42 UT, peaks at 09:44 UT, and ceases at ~10:10 UT. Comparing the flare HXR burst profile and the CME acceleration profile (cf. Fig. 2, *bottom*) we find that both curves are closely synchronized, with the derived start, end and peak times differing by certainly less than 5 minutes.

Figure 3 shows the $d(t)$, $v(t)$, and $a(t)$ curves derived for the CME of 2006 July 6. The impulsive CME acceleration starts at 08:16–08:18 UT, peaks at 08:20 UT with $a = 1.1 \pm 0.5$ km s^{-2}, and has already ended at 08:54 UT when we first observe the CME in LASCO C2. It is important to note that in this event, the main CME acceleration phase is fully covered by the *TRACE* and EIT observations and is finished before the CME appears in the FOV of the LASCO coronagraphs. The *RHESSI* 30–50 keV HXR flux of the associated M2.5 flare starts to increase around 08:18 UT, peaks at 08:23 UT, and is ceased at ~08:40 UT. Again, the CME acceleration profile is tightly synchronized with the HXR flux of the associated flare, and onset and peak times are simultaneous within a few minutes.

5. DISCUSSION AND CONCLUSIONS

We studied two fast CMEs where we could identify CME signatures in on-disk images (SXI, *TRACE*) with high time cadence during the impulsive acceleration phase, and where we also had full HXR coverage of the associate flare's impulsive phase. The derived kinematical curves for both events smoothly continue from on-disk to LASCO observations and the morphology of all the CME signatures measured in the different data sets are very similar (see Fig. 1). In addition, for the 2006 July 6 event the major part of the impulsive acceleration phase had finished before the CME appeared in C2; i.e., the kinematical and dynamical curves are derived from homogeneous data sets (*TRACE* 171 Å and EIT 195 Å), and we can exclude that the derived velocities and accelerations

[1] We note that projection effects only result in a multiplication factor (e.g., Vršnak et al. 2007) and do not alter the profile of the derived kinematical curves.

are artificial due to connecting different features when combining different data sets.

Figures 2 and 3 (*top panels*) reveal a slow rise phase of the CME before the onset of fast acceleration along with the occurrence of HXR bursts. Such a behavior is well known, and the importance of this transition phase was outlined in several studies (e.g., Ohyama & Shibata 1997; Zhang et al. 2001; Sterling & Moore 2005; Isobe & Tripathi 2006; Chifor et al. 2006). As commonly explained (e.g., Forbes 1990), before tearing instability and, hence, fast reconnection below the solar eruption can set in, the current sheet first has to become sufficiently long (slow rise phase).

For both events under study, we found a tight synchronization between the CME acceleration and the HXR profile of the related flare; onsets as well as peaks occur simultaneously within $\lesssim$5 minutes, which is consistent with the observational limitations (time cadence and early detectability of the CME). Since the flare HXR flux is directly related to the number and energy distribution of electrons accelerated during a flare, and since a large fraction of the flare energy goes into fast particles (e.g., Dennis et al. 2003; Emslie et al. 2005), our results provide strong evidence for a feedback relationship between the large-scale CME acceleration and the energy release in the associated flare (see also Zhang et al. 2004). Such a feedback relationship is naturally established by magnetic reconnection occurring in a current sheet behind the CME, as envisaged in the standard flare/CME picture. On the one hand, magnetic reconnection adds poloidal flux to the CME sustaining the Lorentz force which drives the CME acceleration (Chen 1996; Chen & Krall 2003; Vršnak et al. 2004). On the other hand, the higher the acceleration of the CME, the larger the space that is evacuated per unit time in the coronal region behind. This has to be compensated by a stronger mass inflow into the reconnection region (see Shibata & Tanuma 2001 and references therein), which, in turn, causes stronger magnetic reconnection in the current sheet beneath, i.e., stronger flare energy release.

At the end of the CME main acceleration phase both events show a strong decrease of the flare HXR flux. For the 2005 January 17 event it is interesting to note that the acceleration profile and HXR light curve are very similar, even in the late phase when the CME is seen in C2. This indicates that during the impulsive acceleration phase it is the Lorentz force that mainly drives the CME. As the electric current in the erupting system decreases as the CME expands and propagates out from the Sun, the Lorentz force weakens and the drag force owing to the solar wind becomes important (e.g., Cargill et al. 1996; Chen 1996; Vršnak et al. 2004).

In statistical studies the CME velocity was found to be related with the SXR peak flux (e.g., Moon et al. 2002; Burkepile et al. 2004; Vršnak et al. 2005). Here we derived that the CME with the stronger acceleration was associated with a stronger energy release (2005 January 17). However, this is not a universal relation, which might indicate that the flare energy release is not always the dominant factor that determines the CME acceleration (see Maričić et al. 2007).

For the 2005 January 17 CME, the peak acceleration occurs at a plane-of-sky distance from Sun center of 0.9 $R_\odot$, the end of the impulsive acceleration at ~4.9 $R_\odot$. In the 2006 July 6 CME, the peak acceleration occurs at a distance of 0.8 $R_\odot$. The end of its impulsive acceleration occurs below 2.9 $R_\odot$, i.e., is already finished when we first observe the CME in LASCO C2. In both cases, the peak of the impulsive CME acceleration occurs at distances <1 $R_\odot$, i.e., when the CME is still viewed against the solar disk. This implies that for front-sided, fast halo CMEs—by far the most relevant ones in terms of geo-effectivity—it is important to identify CME structures against the solar disk, i.e., in noncoronagraphic images, to properly study their acceleration phase. Presently, coronagraphic observations of the low corona are performed by Mauna Loa MK4 (FOV: 1.08–2.85 $R_\odot$) and the two *STEREO* coronagraphs SECCHI/COR1 (FOV: 1.4–4 $R_\odot$). However, to fully cover the impulsive acceleration phase of fast halo CMEs it is important to have noncoronagraphic observations of early CME signatures as well as spectroscopic observations, since the line-of-sight velocity is more significant in on-disk events (Morimoto & Kurokawa 2003).

We thank the anonymous referee for helpful suggestions and constructive comments that improved the manuscript. We thank the *TRACE*, *SOHO*, *RHESSI*, and *GOES* teams for their open data policy and for supporting our JOP176. We acknowledge support by the Austrian *Fonds zur Förderung der wissenschaftlichen Forschung* (FWF grants J2512-N02 and P15344), the Slovak Research and Development Agency (APVV-0066-06 and APVV-SK-AT-00706), and ISSI-Bern (PI: Giannina Poletto).

REFERENCES

Alexander, D., Metcalf, T. R., & Nitta, N. V. 2002, Geophys. Res. Lett., 29, 41
Brueckner, G. E., et al. 1995, Sol. Phys., 162, 357
Burkepile, J. T., et al. 2004, J. Geophys. Res. Space Phys., 109, 3103
Cargill, P. J., et al. 1996, J. Geophys. Res., 101, 4855
Chen, J. 1996, J. Geophys. Res., 101, 27499
Chen, J., & Krall, J. 2003, J. Geophys. Res. Space Phys., 108, 2
Chifor, C., et al. 2006, A&A, 458, 965
Dauphin, C., Vilmer, N., & Krucker, S. 2006, A&A, 455, 339
Delaboudinière, J.-P., et al. 1995, Sol. Phys., 162, 291
Dennis, B. R., et al. 2003, Adv. Space Res., 32, 2459
Dere, K. P., et al. 1997, Sol. Phys., 175, 601
Emslie, A. G., et al. 2005, J. Geophys. Res. Space Phys., 110, 11103
Forbes, T. G. 1990, J. Geophys. Res., 95, 11919
———. 2000, J. Geophys. Res., 105, 23153
Gallagher, P. T., Lawrence, G. R., & Dennis, B. R. 2003, ApJ, 588, L53
Handy, B. N., et al. 1999, Sol. Phys., 187, 229
Hill, S. M., et al. 2005, Sol. Phys., 226, 255
Hudson, H. S., Acton, L. W., & Freeland, S. L. 1996, ApJ, 470, 629
Isobe, H., & Tripathi, D. 2006, A&A, 449, L17
Kahler, S. W., et al. 1988, ApJ, 328, 824
Kim, Y.-H., et al. 2005, ApJ, 635, 1291
Lin, R. P., et al. 2002, Sol. Phys., 210, 3
MacQueen, R. M., & Fisher, R. R. 1983, Sol. Phys., 89, 89
Maričić, D., et al. 2007, Sol. Phys., 241, 99
Moon, Y.-J., et al. 2002, ApJ, 581, 694
Morimoto, T., & Kurokawa, H. 2003, PASJ, 55, 505
Ohyama, M., & Shibata, K. 1997, PASJ, 49, 249
———. 1998, ApJ, 499, 934
Shibata, K., & Tanuma, S. 2001, Earth, Planets, Space, 53, 473
St. Cyr, O. C., et al. 1999, J. Geophys. Res., 104, 12493
Sterling, A. C., & Moore, R. L. 2004, ApJ, 613, 1221
———. 2005, ApJ, 630, 1148
Temmer, M., et al. 2007, ApJ, 654, 665
Uralov, A. M., Grechnev, V. V., & Hudson, H. S. 2005, J. Geophys. Res. Space Phys., 110, 5104
Veronig, A. M., et al. 2006, ApJ, 647, 1466
Vršnak, B. 2001, J. Geophys. Res., 106, 25249
Vršnak, B., Sudar, D., & Ruždjak, D. 2005, A&A, 435, 1149
Vršnak, B., et al. 2004, A&A, 423, 717
———. 2006, A&A, 448, 739
———. 2007, A&A, 469, 339
Zhang, J., & Dere, K. P. 2006, ApJ, 649, 1100
Zhang, J., et al. 2001, ApJ, 559, 452
———. 2003, ApJ, 582, 520
———. 2004, ApJ, 604, 420